Optimisation of the Friability Property of Sand Moulds Produced by the Binder-Jetting Process

Jonathan Kabadjundi Kabasele
University of Johannesburg, Johannesburg, Gauteng, South Africa

Kasongo Didier Nyembwe
Cape Peninsula University of Technology, Cape Town, Western Cape, South Africa

ABSTRACT

Unlike traditional sand moulding techniques, the binder-jetting process is based on layer-by-layer manufacturing, which significantly influences the cohesion of sand grains and the final friability of the sand moulds. The latter property is critical as it is responsible for the presence of sand inclusions in the final casting and thus the mechanical properties. The friability property of 3D printing has not been systematically investigated and reported upon in metalcasting and foundry literature. This study assesses the friability of three-dimensional AFS sand test specimens produced using the binder-jetting process. In addition, the study attempts to model and optimise the friability property using the central composite design, a response surface methodology in Design-Expert,® to optimise two critical parameters of the binder jetting printer including the grain size and printhead speed to minimise the friability property of sand moulds. The experiment revealed that the quadratic and cubic models of optimisation are the best fit for the correlation. The lowest values of the friability were achieved when the AFS value is closer to 55 in the quadratic model and between 57 and 55 AFS in the cubic model while the ideal value of the printhead speed is above 0.29 mm/s for both models.

Keywords: rapid sand casting, binder jetting, model optimisation, additive manufacturing, sand moulding

INTRODUCTION

Rapid sand casting is the integration of 3D sand printing or binder jetting in the traditional sand casting process. Simply put, in rapid sand casting, the binder jetting process is used to produce moulds instead of traditional moulding methods. Binder jetting (often associated with rapid sand casting) is an additive manufacturing process that involves selectively depositing a liquid binder onto layers of sand to form a mould or core. This technology allows for the rapid creation of complex shapes without the need for traditional patterns and tooling, which is typical in traditional sand casting.[1]

Rapid sand casting offers several advantages. First, it supports a wide variety of materials, providing the potential to surpass other additive manufacturing processes due to compatibility with various powdered substances and binding liquids. The process is relatively simple, as it operates at ambient temperature, avoiding issues like oxidation and residual stress, making the powder highly recyclable and reducing material costs. Additionally, binder jetting enables the production of parts in a broad size range without the need for expensive sealed chambers. The volume of production is high, making it ideal for businesses requiring large quantities of complex parts.[2,3]

The binder jetting process differs from the traditional method of moulding. The introduction of printing parameters and the growth of the part layer by layer with no compaction are distinctive characteristics of the binder jetting process with the potential to affect moulding properties. These differences have prompted several studies on the aggregates suitable for 3D sand moulding and the properties of the 3D printed sand mould. Recent interesting research on rapid sand casting include:

The study by Tshabalala et al., “Optimisation of a resin-coated chromite sand for rapid sand casting applications,” which explored the suitability of South African chromite sand for binder jetting sand printing and further optimise the coating of chromite sand.[4]

Another study investigated the thermal properties of 3D printed sand moulds. It reported that there are differences observed between moulds produced by binder jetting and traditional moulding. As a result, the existing database for traditional moulds found in simulation software had to be upgraded, to properly predict the temperature gradient in moulds produce by binder jetting.[5]

BINDER JETTING PROCESS

Figure 1 depicts part of typical binder jetting which includes a job box having a actuatable build plate therein; a supply box having a bottom platform that is actuatable within the supply box; a printing system including at least one print head connected to a binder source and configured to apply a pattern of binder onto an exposed powder layer over the build plate of the job box; a recoat

system including a recoater configured to move from the supply box to the job box to transfer powder from the supply box to the job box so as to form a new powder layer over the build plate of the job box; and a cure system configured to direct electromagnetic radiation onto the job box.[1]

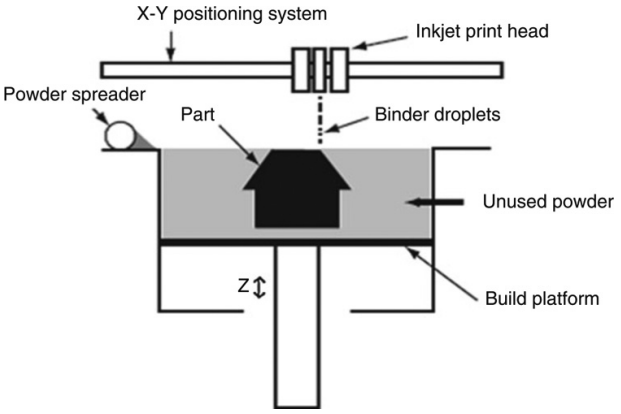

Figure 1. Schematic of a binder jetting printer.[1]

In 3D printing, two main types of printheads are commonly used to generate liquid binder drops: drop-on-demand (DoD) and continuous-jet (CJ) printheads. The DoD printheads work by producing individual drops only when needed. Among these, two common technologies are piezoelectric and thermal inkjet printheads. Piezoelectric printheads create droplets by changing the shape of a small chamber using piezoelectric materials, which forces the liquid out. The Voxeljet VX1000 printer, which was used in this work, features a high-precision piezoelectric printhead, is well-suited for printing complex parts of varying designs and shapes, offering versatility for different applications.[6]

PARAMETERS OF BINDER JETTING PRINTERS

The process parameters of 3D sand printer include printhead speed, recoater speed, drop mass (binder concentration), print resolution X, Y and Z, catalyst, or activator concentration.[7,8]

The recoater speed is a parameter that describes how fast the premixed sand is laid out by the recoater on the building platform.[5,6]

The X, Y and Z resolutions describes the minimum distance after which the print head nozzles spread the binder droplet on demand over the previous layer of sand. In some cases, the resolutions are kept constant, this is the case for the ExOne S-printer where the value of the Y resolution is kept constant at 101,6 µm. Which means that for this printer the inkjet nozzles are kept at a constant distance in the Y direction. The Z direction can be determined by the sand layer thickness, this implies that the Z resolution is strongly related to the sand particle size. It is important to note that, the X resolution is a distance that regulates the number of times the binder is jetted by the printhead per unit length. Thus, the resolution X correlates with the concentration of binder. Simply put, a shorter resolution X increases the amount of resin required to produce moulds.[5,6]

Layer thickness refers to the thickness of each individual layer of sand in a mould produced by binder jetting. The activator or catalyst used in this case is an arylsulphonic acid in conjunction with furan binder.[7,8]

The binder print orientation refers to the direction in which the binder is applied to the sand layer, either vertical or horizontal.[9]

Table 1 provide a comprehensive description of all the parameters of a typical binder jetting printer.

Table 1. Description of Binder Jetting Printer Parameters

Parameters	Description
Printhead Speed	The speed at which the printhead moves across the build platform to deposit binder droplets.
Recoater Speed	The speed at which the recoater lays out the premixed sand on the building platform.
Drop Mass (Binder Concentration)	The concentration of binder in the droplets dispensed by the printhead.
Print Resolution X	The minimum distance between binder droplets spread by the printhead in the X direction.
Print Resolution Y	The minimum distance between binder droplets spread by the printhead in the Y direction (e.g., constant at 101.6 µm for ExOne S-printer).
Print Resolution Z	The thickness of each sand layer deposited (related to sand particle size and layer thickness).
Activator or Catalyst Concentration	The concentration of activator or catalyst (e.g., arylsulphonic acid) used in conjunction with the binder.
Binder Print Orientation	The direction in which the binder is applied to the sand layer, either vertical or horizontal.

There is ongoing research on the parameter of binder jetting printer that are providing insight into the process. Notable research on the topic was conducted by Foo et al. who reported in their studies that varying the binder print orientation introduces differences in the severity of thermal distortion supporting the hypothesis that process

parameters of binder jetting may in fact alter the thermo-mechanical and by extension, the properties of the casting. Other studies reported that varying the recoater speed, print resolution, layer thickness and activator concentration has impact on the mechanical properties of the mould, gas emissions,[9] these publications further reinforce the existing disparities between the binder jetting process and traditional methods of moulding.

SAND MOULD EROSION AND SAND INCLUSIONS

Friability is a measure of the surface integrity of the mould. A high friability test value percentage indicates a mould with poor cohesion and is undesirable for casting applications. In contrast, a low percentage of friability test result indicates good bonding strength and better resistance to the erosive force from the liquid metal. Many studies have reported that fine sand, fillers, hard ramming, and mould paints contribute to the prevention of mould erosion. Mould coating has proven to be an effective method of improving friability.[10]

Mould erosion is favoured by poor friability because of poor sand ramming.[10] Erosion in sand moulds is caused by the mechanical effect of molten metal impacting the mould and the thermal effect of heat transfer. The severity of erosion is affected by factors such as the angle of metal jet incidence, moulding sand compaction, and temperature of the molten metal.[10]

Sodium silicate-bonded sands show higher resistance to erosion. However, these sands may result in rougher casting surfaces due to the destruction of sand grain bonds, which can be mitigated by using protective coatings such as zirconium oxide-based coatings and higher compaction levels.[11]

To mitigate the turbulent flow of the metal gating system, a bottom-up pouring method helps in alleviating the mould erosion by reducing the metallostatic pressure of the metal on the mould wall.[11]

A major consequence of poor friability and mould erosion is sand inclusions in the casting. Sand inclusions in castings result in several detrimental effects due to the entrapment of sand particles within the metal matrix. These inclusions not only cause surface defects, such as rough patches or indentations, but also weaken the structural integrity of the casting. When sand particles become trapped in the metal matrix, they act as stress concentrators, disrupting the uniformity of the material and creating points of weakness. This leads to a higher risk of premature failure, cracking, or fractures under load, particularly in high-stress environments. The trapped inclusions also reduce the casting's fatigue resistance, a critical issue in industries where components are subject to cyclic loading, such as automotive and aerospace sectors. In addition to these structural concerns, sand inclusions complicate machining processes by creating hard spots that wear down cutting tools, increasing operational costs. Ultimately, castings with significant inclusions often fail to meet quality standards, leading to rejection, rework, and higher production costs.[11]

The absence of compaction in 3D sand printing and the introduction of new process parameters have the potential to introduce variability on the friability of the 3D sand mould, putting the casting at risk of sand inclusion and tremendous loss for founders.[10]

Thus, the aim of this work is to study the friability of 3D sand mould while varying the parameters of the print namely the printhead speed and the grain size of the sand and identify how the different combination of parameter will affect the friability. In addition, the data will be used to develop an optimisation model with the objective of minimising the friability percentage of mould using the response surface methodology. The friability test described in the AFS standard will be used in the current work.

METHODOLOGY

The experimental procedure is described in Figure 2. The procedure includes four steps namely sand sampling, sand characterisation, mould printing by binder jetting at varying printhead speed, friability testing and numerical optimisation.

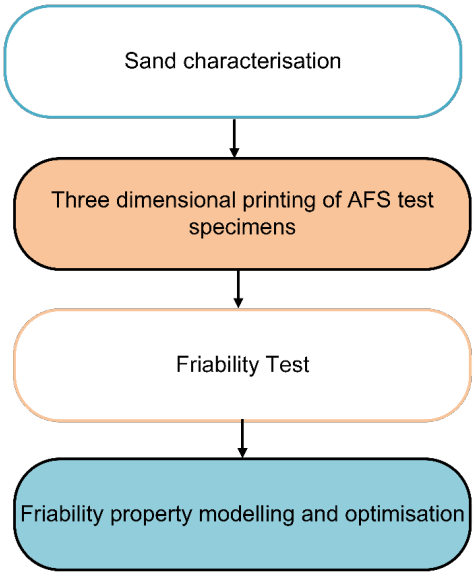

Figure 2. The experimental procedure.

In step one, four samples of foundry silica sand with different grain size were acquired from a supplier in South Africa. The sieve grading test reported values of 58, 65, 55 and 64.5 AFS. Table 2 provides detailed descriptions of the samples.

Table 2. Silica Sand Samples

Silica sand samples	AFS value	Quantity
Sample 1	58.0	1 ton
Sample 2	65.0	1 ton
Sample 3	55.0	1 ton
Sample 4	64.5	1 ton

The printing of the test specimen took place in the second step. First, the sand was coated with an acid catalyst. The equipment is a prototype developed at the Vaal University of Technology. The printer used was a Voxeljet VX1000, the varying parameters of the print is the speed of the printhead in mm/s, the other parameter is the grain size which was determined as being different across the various samples.

The printhead speed was selected because it is a major parameter of the 3D sand printer by having an important impact on several aspect of the process. Printhead speed in 3D sand printing affects several critical aspects of the process. Higher speeds can reduce layer precision, resulting in lower surface finish and dimensional accuracy, while slower speeds allow for finer detail and better quality. Faster speeds may also lead to weaker adhesion due to less binder deposition, whereas slower speeds improve part strength by allowing more time for binder application. Although increasing speed enhances production efficiency, it can compromise quality if not balanced with other factors like binder flow rate. Additionally, faster speeds reduce binder consumption but can lead to under-saturation and weaker parts, while also affecting the control over layer thickness and uniformity.[12,13] Another reason for selecting printhead speed is that it was the only parameter adjustable in accordance with the OEM's (original equipment manufacturers) recommendations.

The printhead speed varied between 0.0106 in/s to 0.028 in/s (in. 0.27 to 0.72 mm/s) and the grain size varied between 58 and 65 AFS. The printed AFS test specimen (2 in. diameter x 2 in. height) were all heat cured. Figure 3 shows the laboratory equipment used, including the sand coating machine, coated sand, printed sand moulds and 3D printer. Table 3 describes the combination of printer parameters.

In the third step of the experimental procedure, the printed test specimens shaped as cylinders with dimensions 2 in. diameter x 2 in. height (50mm height x 50 mm diameter) are tested in the friability tester.

Figure 3. Laboratory equipment and materials used in this study included the sand coating machine, coated sand, printed sand moulds and 3D printer.

Table 3. Printer Parameters and Corresponding AFS Grain Fineness

Printhead Speed (mm/s)	AFS Grain Fineness
0.72	64.50
0.65	64.50
0.65	55.00
0.61	64.50
0.27	55.00
0.54	58.00
0.61	58.00
0.61	55.00
0.65	65.00
0.54	55.00
0.72	58.00
0.72	65.00
0.54	65.00

Two samples are placed next to each other inside the rotating drums. The machine is set to rotate at 57 RPM for 1 min according to the AFS 2248-11-S Standard. The samples rub against each other as the as the rotating drums makes the rotational motion. The eroded sand falls

off the rotating drum and is collected on a paper. The eroded sand is measure on the scale and the friability percentage is obtained by the ratio of the eroded sand to the original mass. The test equipment used (Figure 4) is a prototype developed at the Vaal University of Technology.

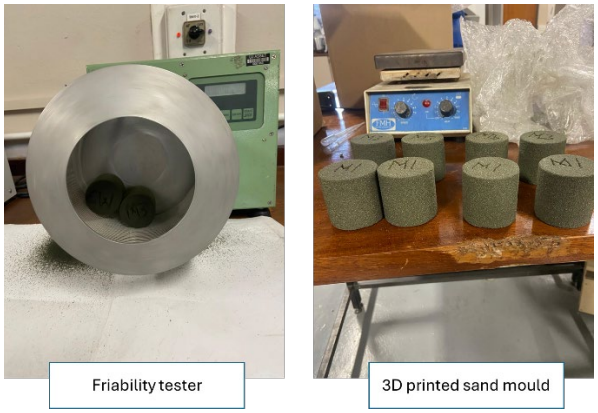

Figure 4. Friability test equipment and the 3D printed sand moulds are shown.

The central composite design, a Response Surface Methodology, is used to optimise the process by generating models that minimise the value of the friability percentage. The software used, was Design Expert® (Version 7.0.0).

Central Composite Design (CCD) is a popular experimental design used in Response Surface Methodology (RSM) for exploring the relationship between multiple input parameters and the response variable. Its primary purpose in parametric optimisation is to build a quadratic model, helping to identify optimal settings of the parameters to either maximise or minimise a response.

RESULTS

FRIABILITY TEST

The results of the friability test are recorded in Table 4. The lowest value of friability recorded was 11.49% (when AFS value = 55 and printhead speed = 0.27 mm/s) and 14.44 % (when AFS value = 55 and printhead speed = 0.54 mm/s). The highest recorded values of the friability percentage were 42.15 (when AFS value = 58 and printhead speed = 0.72 mm/s) is 43.83% (when AFS value = 58 and printhead speed = 0.61 mm/s).

These values of friability were very poor and uncommon in traditionally moulded specimens. In general, a 10% friability is targeted to produce sound castings with good mechanical properties. It is important to note that the lowest values are better than those reported in the literature.[14] Nyembwe et al., obtained best values of 16% for the test specimen produced with the standard parameters recommended by the OEM. The poor performance of the 3DP sand mould in terms of friability compared to traditional moulding methods was generally attributed to the quasi absence of compaction during the layer-by-layer manufacturing.

Table 4. Test Results for Actual Experimental Work

Printhead Speed (mm/s)	AFS Grain Fineness	Friability %
0.72		36.42
0.65	**64.5**	38.24
0.61		40.71
0.65		19.01
0.27		11.49
0.61	**55**	17.81
0.54		14.44
0.54		31.11
0.61	**58.00**	43.83
0.72		42.15
0.65		36.42
0.72	**65**	29.05
0.54		38.26

NUMERICAL OPTIMISATION

The optimisation process is performed by central composite for response surface methodology in the Design of Experiment software.

Table 5 showcases a different model that the software uses to define the correlation between the response variables and the predictor in a sequential sum of squares. The sequential sum of squares partitions the total variation in the data into portions attributable to different sources (factors, variables) based on the sequence in which they are entered into the model. This helps to understand how much of the variation in the data is explained by the model. The main parameters to consider for the validation of the model in a sequential model of squares are the degrees of freedom (df), the F value and the p-value.

The degrees of freedom (df) determine the flexibility of the model and is used to adjust the sum of squares to

obtain the mean squares. Higher degrees of freedom typically indicate more reliable estimates. In this case the cubic and quadratic model have the highest df with respective values of 4 and 2 (Table 5).

The F-value tests the overall significance of the model. A higher F-value suggests that the model provides a better fit than a model with no predictors. According to the results recorded in Table 6, the quadratic model has the highest F- value of 18.15 (Table 5).

The p-value assesses the significance of individual factors. A low p-value indicates that the factor significantly contributes to explaining the variability in the dependent variable. The quadratic model has the smallest p-value of 0.0017 (Table 5).

Table 6 provides more information about the selection process of a suitable model. The main parameters to consider are the standard deviation, R^2, adjusted R^2 and predicted R^2.

The standard deviation of the residuals (errors) in a model is a measure of how spread out the residuals are. It indicates the average distance between the observed values and the model's predicted values. A smaller standard deviation means that the model predictions are closer to the observed data points, indicating a better fit. The quadratic and cubic model have the lowest standard deviation with respective value of 3.62 and 1.9. However, a small standard deviation alone does not guarantee a good model; it must be considered in conjunction with other statistics like R^2 (Table 6).

R^2 measures the proportion of the variance in the dependent variable that is explained by the independent variables in the model. The quadratic and cubic models have a R^2 value close to 1, 0.9397 and 0.9929 respectively, indicating that the models explain most of the variability in the dependent variable (Table 6).

Adjusted R^2 is more useful than regular R^2 in models with multiple predictors because it discourages overfitting. A higher Adjusted R^2 indicates that the model performs better by accounting for the number of predictors. Both quadratic and cubic models have the highest Adjusted R^2 with respective values of 0.8966 and 0.9716 (Table 6).

Predicted R^2 measures how well the model is likely to predict new data. Unlike Adjusted R^2, which adjusts for the number of predictors, Predicted R^2 is based on how well the model predicts responses for data points that were not used to fit the model. A large difference between Adjusted R^2 and Predicted R^2 is observed for both quadratic and cubic models, suggesting overfitting. The models may fit the training data well but perform poorly on new data (Table 6).

The Prediction Error Sum of Squares (PRESS) is used to assess the predictive ability of the model. A lower PRESS value suggests that the model has better predictive power. The cubic model has a relatively low PRESS value of 632.92, highlighting a relatively better predictive power (Table 6).

Considering all the information gathered from the Response Surface Methodology, the quadratic and cubic models were considered to explain the correlation between the predictors (printhead speed and AFS grain fineness) and the response (percentage of friability).

Figures 5 and 6 highlight the 3D surface graphical representation of the quadratic and cubic models, respectively.

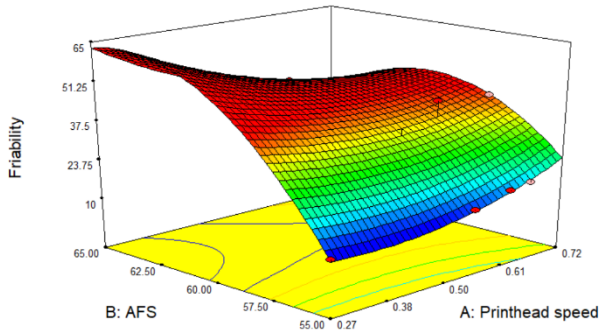

Figure 5. The 3D surface graphical representation of the quadratic model.

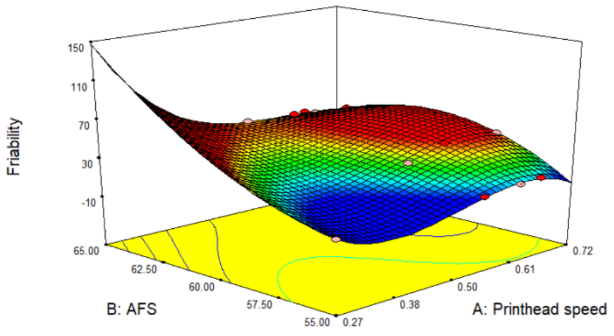

Figure 6. The 3D surface graphical representation of the cubic model.

Table 5. Sequential Model Sum of Squares

Source	Sum of Squares	df	Mean Square	F Value	p-value Prob > F	
Mean vs. Total	12242.55	1	12242.55			
Linear vs. Mean	812.07	2	406.03	5.72	0.0221	
2FI vs. Linear	142.29	1	142.29	2.25	0.1674	
Quadratic vs. 2FI	476.1	2	238.05	18.15	0.0017	Suggested
Cubic vs. Quadratic	80.98	4	20.24	5.61	0.094	Suggested
Residual	10.82	3	3.61			
Total	13764.8	13	1058.83			

Table 6. Model Summary Statistics

Source	Standard Deviation	R^2	Adjusted R^2	Predicted R^2	PRESS	
Linear	8.43	0.5335	0.4402	0.2619	1123.55	
2FI	7.94	0.6269	0.5026	0.0001	1522.13	
Quadratic	3.62	0.9397	0.8966	-1.5884	3940.2	Suggested
Cubic	1.9	0.9929	0.9716	0.5842	632.92	Suggested

The equations of the quadratic model (Equation 1) and cubic model (Equation 2) will be used to determine the best set of parameters that will produce the least percentage of friability.

$$\begin{aligned}Friability = {} & -3019.55668 \\ & + (462.99671 * \text{Printhead speed}) \\ & + (95.50144 * AFS) \\ & - (9.75845 * \text{Printhead speed} * AFS) \\ & + (105.47026 * \text{Printhead speed}^2) \\ & - (0.73056 * AFS^2)\end{aligned} \quad \textbf{Eqn. 1}$$

$$\begin{aligned}Friability = {} & + 6563.79600 \\ & - (14475.14163 * \text{Printhead speed}) \\ & - (242.16807 * AFS) \\ & + (513.99930 * \text{Printhead speed} * AFS) \\ & - (578.11062 * \text{Printhead speed}^2) \\ & + (2.33160 * AFS^2) \\ & + (92.85792 * \text{Printhead speed}^2 * AFS) \\ & - (5.25623 * \text{Printhead speed} * AFS^2) \\ & - (3045.99340 * \text{Printhead speed}^3) \\ & + (7.24979E\text{-}005 * AFS^3)\end{aligned} \quad \textbf{Eqn. 2}$$

Table 7 provides the set of parameters that produce the best friability results. Ideally the mould must have a friability of 10% to be deemed acceptable. The lowest value achieved with these set of parameters is 11.49%.

Table 7. Ideal Set of Parameters

Model	AFS	Printhead speed (mm/s)
Quadratic	55.01 – 55.11 (55)	0.29 – 0.69
Cubic	55.23 – 57.98	0.31 – 0.72

KEY FINDINGS AND FUTURE WORK

The experiments revealed that the cubic and quadratic model are the best fit for the correlation between the predictor (namely printhead speed and AFS grain fineness) and the response (friability percentage). The lowest value of friability is achieved when the AFS value is closer to 55 in the quadratic model and between 57 and 55 in the cubic model while the ideal value of the printhead speed is above 0.29 mm/s for both models.

Previous research examined the properties of 3D sand printed moulds, with reported friability values close to 16%.[14] In contrast, the present study observed significantly higher friability results, reaching around 43%, which exceeds the recommended limits with the potential to affect the casting with sand inclusions causing a serious risk to the structural integrity of the final

product. However, friability percentages below 16% were also achieved, highlighting the critical role of process optimisation and modelling in 3D sand printing and rapid sand casting.

The authors acknowledge the limitations of the models that were built to optimise the friability of 3D sand moulds, particularly their struggles with overfitting and restricted predictive capabilities.[15] This study represents a preliminary step in a larger, ongoing effort to refine these models. Future research will aim to expand the dataset significantly, providing a stronger foundation for improved accuracy and generalizability. Moreover, the team intends to explore the influence of additional 3D printing process parameters on the friability of foundry moulds, paving the way for a deeper understanding and enhanced optimisation of the process.

CONCLUSIONS

The current study on the optimisation of the technology of binder jetting serve as a foundation for the broader adoption of the technology in foundries across the world. The quick rise of rapid sand casting places this new technology in a unique position to drive the industry forward embracing customisation, high complexity of parts and cost effectiveness. This study revealed that the friability property of the mould produced by binder jetting is inferior to traditional moulds. The optimisation of friability using specialized software identified the optimal combination of sand granulometry and printhead speed to minimise the friability of binder-jetting sand moulds, paving the way for more robust models that will bring the friability of 3D sand printed moulds closer to that of traditional sand moulds.

ACKNOWLEDGMENTS

The author thanks the Collaborative Program for Additive Manufacturing (CPAM). Special thanks to the University of Johannesburg and the Vaal University of Technology.

REFERENCES

1. T.A.L. Neel, P. Mognol and J.-Y. Hascoet, "A review on additive manufacturing of sand moulds by binder jetting and selective laser sintering," *Rapid Prototyping Journal*, vol. 24, no. 8, pp. 1325-1336 (2018).
2. P. Saxena, E. Pagone, K. Salonitis and M.R. Jolly, "Sustainability metrics for rapid manufacturing of the sand casting moulds: A multi-criteria decision-making algorithm-based approach," *Journal of Cleaner Production*, vol. 311, no. 1, pp. 127506-127517 (2021).
3. M. Upadhyaya, T. Sivarupana and M.E. Mansoria, "3D printing for rapid sand casting—A review," *Journal of Manufacturing Process*es , vol. 29, no. 1, pp. 211-220 (2017).
4. N. Tshabalala, K. Nyembwe and P.V. Tonder, "Optimisation of a resin-coated chromite sand for rapid sand casting applications," *South African Journal of Industrial Engineering*, vol. 32, no. 3, pp. 290-298 (2021).
5. M. Saeidpour, R. Svenningsson, U. Gotthardsson and S. Farre, "Thermal Properties of 3D-Printed Sand Moulds," *International Journal of Metalcasting*, vol. 16, no. 1, pp. 252-258 (2022).
6. S.F. Pond, Inkjet technology and product development strategies (2000).
7. T. Sivarupan, M.E. Mansori, N. Coniglio and M. Dargusch, "Effect of process parameters on flexure strength and gas permeability of 3D printed sand moulds," *Journal of Manufacturing Processes*, vol. 54, no. 1, pp. 420-437 (2020).
8. G. Gao, W. Zhang, Z. Du, Q. Liu, Y. Su and D. Shi, "Investigation of selected parameters effect on 3D printed sand mould properties through Taguchi method," *Rapid Prototyping Journal*, vol. 27, no. 3, pp. 627-635 (2020).
9. J. Foo, S. Ramrattan and R. Tuttle, "Considering the Effects of Thermo-Mechanical Anisotropy in 3D Printed Silica Sands Moulds," *AFS Metalcasting Congress Proceedings*, Cleveland (2023).
10. P. Beeley, “Foundry Technology,” 2nd ed., Oxford: Butterworth-Heinemann (2001).
11. J. Campbell, “Complete Casting Handbook: Metal Casting Processes, Metallurgy, Techniques and Design,” USA: Butterworth-Heinemann (2015).
12. A. Zocca, C.M. Gomes, T. Stauder and J. Günster, "Additive manufacturing of SiSiC by layerwise slurry deposition and binder jetting (BSD-BJ)," *Journal of the European Ceramic Society*, vol. 35, no. 6, pp. 1947-1953 (2015).
13. B. Mersch, C. Seidel and B. Kleemann, "Process influence on mechanical properties and surface roughness in 3D sand printing," *Procedia Manufacturing*, vol. 35, pp. 185-191 (2019).
14. K. Nyembwe, M. Mashila, P.D. Tonder, D.D. Beer and E. Gonya, "Physical Properties Of Sand Parts Produced Using A Voxeljet Vx1000 Three dimensional Printer," *South African Journal of Industrial Engineering*, vol. 27, no. 3, pp. 136–142, (2016).
15. A.R. Ajiboye, R. Abdullah-Arshah, H. Qin and H. Isah-Kebbe, "Evaluating The Effect Of Dataset Size On Predictive Model Using Supervised Learning Technique," *International Journal of Software Engineering & Computer Sciences (IJSECS)* , vol. 1, no. 1, pp. 75-84 (2015).